ANALYSING AND MODELING HIGH TEMPERATURE OXIDATION OF STEEL SLABS DURING REHEATING *

Thomas Höfler[1, 2]
Michael Auinger[3]
Bernhard Linder[4]
Gerhard Angeli[5]
Herbert Danninger[6]

Abstract
Gas-fired pusher furnaces are commonly used to heat steel slabs before hot rolling. Temperatures well above 1000 °C combined with an oxidizing atmosphere containing H_2O, CO_2 and O_2 result in rapid oxidation of most steel grades. The resulting oxide scale and the chemistry of the metal-scale-interface are major determining factors for the occurrence of hot rolling defects. To better understand these phenomena, lab-scale trials were performed with two different steel grades in an electric tube furnace in the temperature range 1000-1250 °C, using an atmosphere of about 20 % H_2O, 7 % CO_2 and 3 % O_2. Humidification of the gas was achieved by evaporation, using a custom thermostat with standard laboratory glassware. The resulting samples were prepared metallographically, using cold mounting under vacuum with taper section angles, and analyzed using light microscopy and SEM/EDS. The scale structure of the Si alloyed steel was highly dependent on the oxidation temperature due to the formation of eutectic liquid phases of FeO, Fe_2SiO_4 and $FeAl_2O_4$. Below the eutectic temperature, the scale of the Si steel appeared to be made up of three distinct areas: The external scale consisting solely of Fe oxides, the internal scale containing Fe_2SiO_4 and $FeAl_2O_4$, and an internal oxidation zone with SiO_2 and Al_2O_3 in a mostly plain Fe matrix. Comparisons of the experimental results with simulations of the internal oxidation showed good qualitative agreement.
Keywords: Steel; Hot Rolling; Oxidation; Simulation

1 *Researcher, K1-MET GmbH, Linz, Austria.*
2 *PhD Student, Institute of Chemical Technologies and Analytics, TU Wien, Vienna, Austria.*
3 *Assistant Professor, WMG, University of Warwick, Coventry, UK.*
4 *Senior Researcher, Business Unit Coil / Research & Development, voestalpine Stahl GmbH, Linz, Austria.*
5 *Senior Researcher, Research & Development, voestalpine Stahl GmbH, Linz, Austria.*
6 *Dean and Full Professor, Institute of Chemical Technologies and Analytics, TU Wien, Vienna, Austria*

1 INTRODUCTION

The formation of oxide scales on steels during hot rolling is virtually inevitable. Residual scale left on slabs after going through descaling as well as chemical changes at the metal-scale-interface present a risk for generation of various defects. Among all the common steel alloying elements, silicon is probably most often described as enhancing rolling defects. Si-alloyed steels are prone to a defect commonly referred to as “red scale”, where residual scale is rolled into the steel, affecting the surface quality of the final product [1]. Nickel is often described as contributing to this effect [2][3].

This paper aims to present experimental methods for reproducing the oxidizing conditions found in common reheating furnaces, guidelines for preparing oxidized samples and help gaining a better understanding how oxide scales are formed, supported by simulations of internal oxidation processes.

2 MATERIAL AND METHODS

The general workflow for the oxidation trials and the following metallographic preparation can be seen in Figure 1. Details are explained in the following sections.

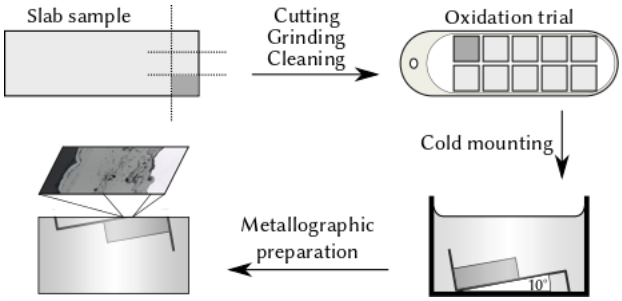

Figure 1. Sample preparation scheme

2.1 Oxidation Experiments

Samples from two different steel grades provided by voestalpine Stahl GmbH in the form of 12 x 4 x 0.5 cm³ pieces cut from as-cast slabs were used. Their compositions are shown in Table 1.

Table 1. Compositions of the steels used [wt. %]

Name	C	Si	Al	Mn	Cr
Si steel	< 0.1	2.4	1.1	0.3	< 0.1
Cr-Mn steel	0.1	0.2	< 0.1	2.2	0.3

Before the experiments, samples were cut to about 1.25 x 1.25 x 0.5 cm³, ground to P2000 grit and cleaned in isopropanol in an ultrasonic cleaner, with the last grinding and cleaning step being performed shortly before the experiment. For each experiment, 10 samples each were placed on fused corundum in a furnace boat (C799) with a length of about 120 mm. The prepared surfaces were facing up, with the gas flowing over them laterally.

When trying to reproduce the conditions found in a gas-fired reheating furnace in a lab-scale electric furnace, two major difficulties arise: First, due to the combustion process, the atmosphere contains approximately 20 % H_2O by volume (depending on the exact composition of the fuel and the air-fuel-ratio) [4], which has a significant impact on the oxidation behavior [5][6]. Corresponding to a dew point of about 60 °C, this implies that all surfaces between the humidification system and the samples have to be heated above this temperature in order to avoid condensation, which is especially harmful when using ceramic furnace tubes. Second, the oxidation rate is dependent on the flow velocity of the oxidizing agent up to a certain point [7]. Especially when oxidizing at higher temperatures with resulting high reaction rates, one has to make certain that enough oxidant is provided to ensure homogeneous oxidation of all samples.

Atmospheres consisting of H_2O, CO_2, O_2 and N_2 are typically either generated by combustion of natural gases [2][8] or by humidifying a premixture of CO_2, O_2 and N_2 to a defined dew point [9]. The latter is

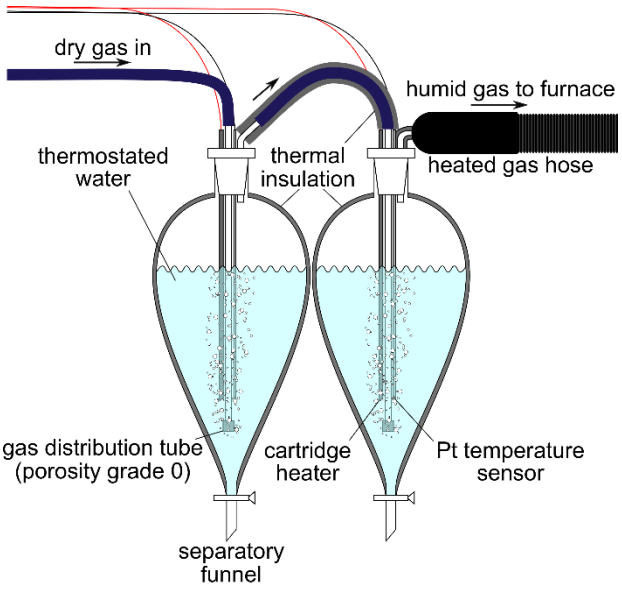

Figure 2. Setup of the gas humidifier.

usually done by passing the dry gas through water held at a constant temperature, which should ideally result in the gas getting saturated to the dew point corresponding to the temperature of the water. This is also the method chosen for this work.

The experimental setup for the humidification system can be seen in Figure 2. A dry gas pre-mix containing about 3.7 % O_2 and 8.7 % CO_2 by volume (balance N_2) is being led through a series of two separatory funnels with thermo-stated water. Proper dispersion of the gas in the liquid is ensured through the use of gas distribution tubes with sintered glass filters with a pore size of roughly 0.25 mm. The water in the first funnel was heated to 2–5 °C above the target dew point, while the second was set to the desired dew point temperature of 60 °C. This results in a slight over-humidification in the first step, so that the exact degree of humidity can be controlled through condensation in the second step. The dew point achieved was checked by determining the mass difference of the water inside the humidifier before and after each experiment. In addition, the amount of water actually transported through the furnace was determined by using a Dimroth-condenser coupled with a gas washing bottle for collecting the condensate behind the furnace.

For transporting the humid gas to the furnace while preventing condensation, a self-regulating heated gas hose with a holding temperature of about 120 °C was employed. The valves allowing switching between different gas types right before the furnace were heated using a resistive heating element, and the temperature of the furnace tube end caps was held constant at 80 °C by connecting them to a laboratory thermostat.

The actual oxidation of the steel samples was performed inside a mullite furnace tube (C610) with an inner diameter of 35 mm within an electrically heated furnace. With a dry gas flow of 6 L/min at room temperature, this results in an average gas velocity of 10.4 cm/s, well above the critical gas velocity of 4.2 cm/s found by Abuluwefa et al. for O_2/N_2 gas mixtures, above which the weight gain rate remains constant [7]. Assuming ideal gas behavior of the humidified gas at 1000 °C, the gas velocity would reach approximately 56.4 cm/s.

Before the experiments, the temperature profile of the furnace under the humid gas flow was determined with a type K thermo-couple. Additionally, profile measurements with ceramic process temperature control rings (PTCR) were performed. The samples were centered according to the measurements. Later experiments also included a single PTCR for verification.

2.2 Metallographic Preparation

For the preparation of the oxidized samples, cold mounting in vacuum is preferable. This helps to ensure that the often fragile scale remains undamaged and porosity is infiltrated, which is beneficial for the following grinding and polishing steps. 10° taper section angles were used to

achieve increased magnification of the different scale layers.

As previously reported by Chen and Yuen [10], extended polishing with 3 µm diamond was found necessary to remove defects introduced in previous preparation steps, which could otherwise be mistaken for genuine porosity. Figure 3 shows the preparation progress using 3 µm diamond starting from a preparation with 9 µm diamond. After polishing for 3 min, there is still a large amount of oxide breakout from the previous grinding and coarse polishing steps visible, especially near the scale surface. Optimal mitigation of the scale damage can usually be expected after about 12-15 min, resulting in clearly defined cracks and strongly reduced porosity from oxide breakout.

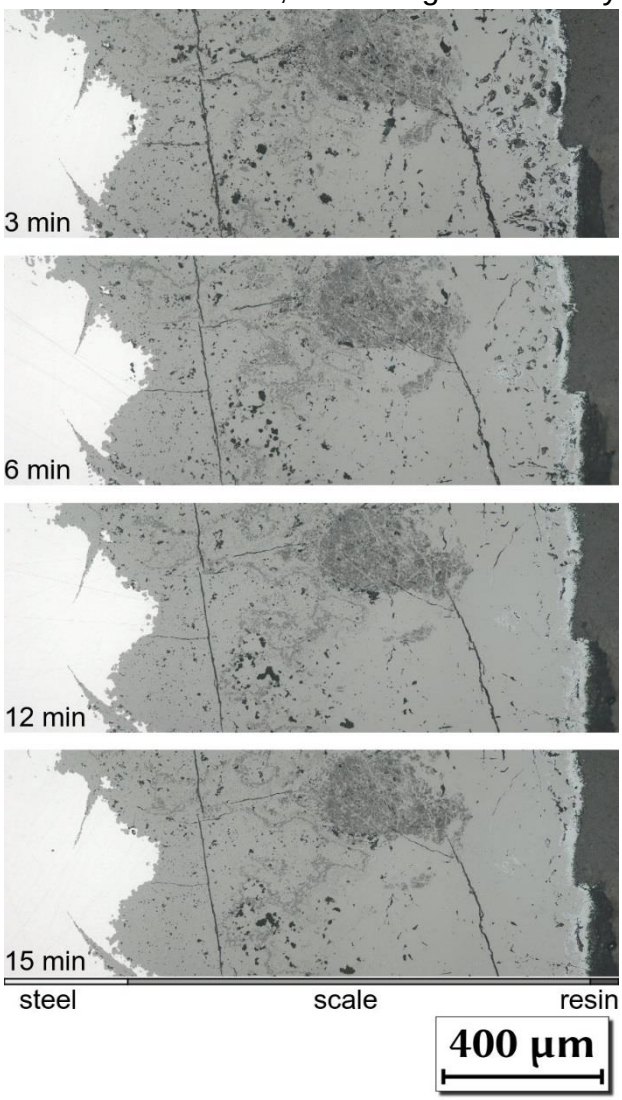

Figure 3. Progress during preparation with 3 µm diamond, cold mounted 10°-taper section.

2.3 Simulation

Previous research on the simulation of internal oxidation in steels has been conducted by Auinger et al. [11] and Bott et al. [12], upon which this work is based on. The formation of oxide scale on steel can be broken down into two sub-processes: diffusion and oxidation reaction. The diffusion of alloying elements and oxygen in the steel can be modeled according to Fick's second law (Equation 1):

$$\frac{\partial c}{\partial t} = D \frac{\partial^2 c}{\partial x^2} \quad (1)$$

Using the implicit Euler method, the above equation can be solved as a system of linear equations for a discrete, one-dimensional grid. Implementation of the simulation was performed in MATLAB.

The reactions for oxidation were predefined according to the various oxides formed by alloying elements. Complete reaction of the diffusing species according to these reactions – sorted by ascending Gibbs energy – was assumed. This assumption was made as the calculation of true equilibria for each time step would have taken much more computational resources.

Furthermore, the model only takes the internal oxidation of base metals in the steel into account. Ion transport through wuestite relies heavily on defects found in its structure [13], and would thus require another approach to model. In the model used for this work, the wuestite/steel interface was assumed as stationary. Furthermore, assuming the diffusion from wuestite into the steel to be the limiting factor for oxygen transport, the boundary concentration at the interface was set to the temperature-dependent solubility limit of oxygen in pure iron [14].

3 RESULTS AND DISCUSSION

3.1 Isothermal and non-isothermal oxidation

The first oxidation trials were performed isothermally: Samples were heated in inert Ar atmosphere up to the holding temperature before flowing the oxidising gas mixture into the furnace. After oxidation, the samples were cooled in Ar inside the furnace with a nominal rate of 10 K/min. However, cooling slowed down and became increasingly nonlinear below 800 °C furnace temperature.

Despite the high gas flow rate of 6 L/min, the appearance of the samples after isothermal oxidation was inhomogeneous, as seen in Figures 4 and 5. In contrast to the thicker, smooth oxides formed on the samples closer to the gas entrance, the samples to the back formed a thinner scale, featuring a coarse, crystalline oxide surface with whiskers (Figure 6). With a reduced gas flow of 2 L/min, the coarse oxide zone extends even further across the samples, suggesting dependence on the oxidizing atmosphere (Figure 7).

Figure 4. Cr-Mn steel before (top) and after (bottom) isothermal oxidation at 1200 °C, 15 min, 6 L/min.

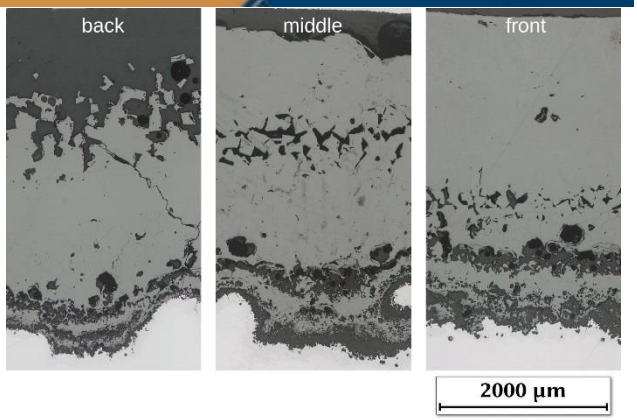

Figure 5. Comparison of scale structures across samples from Figure 4, 10° taper section.

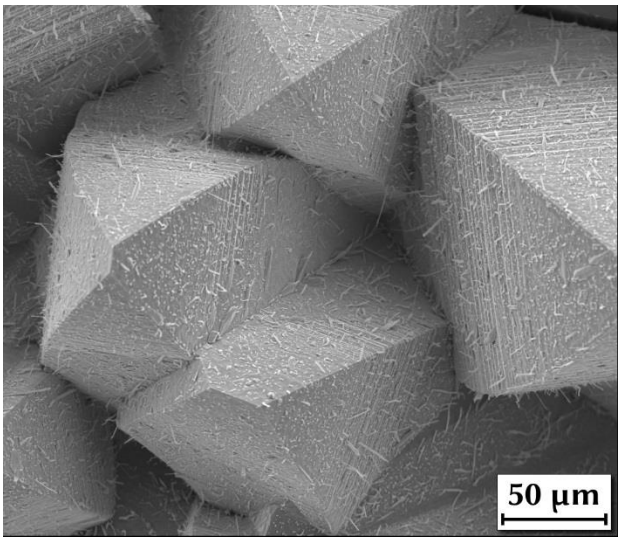

Figure 6. SE image of the coarse oxide surface on the backmost samples in Figure 4.

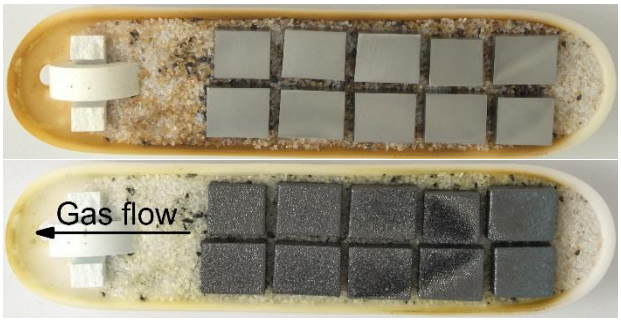

Figure 7. Cr-Mn steel before (top) and after (bottom) isothermal oxidation at 1200 °C, 15 min, 2 L/min.

In order to ensure uniform oxidation of the samples, the experimental setup was changed so that the oxidizing atmosphere could be introduced into the furnace already during the heating period. The assumption was that an even oxide layer would form on all samples during lower temperatures with lower reaction rates. At

the holding temperature, the existing oxide layer should slow down the oxidation, preventing rapid consumption of the oxidizing species by the front samples. However, due to the aforementioned risk of condensation, the humid gas could not be safely lead into the furnace at room temperature. As a result, the furnace was first heated to about 500 °C under inert atmosphere, held for 15 min, and then heated with 10 K/min to the desired isothermal holding temperature while flowing the oxidizing gas into the furnace tube. This resulted in a more even appearance of the oxidized samples (see Figure 8) and had the added benefit of more closely resembling the actual reheating process of steel slabs. Other than blistering occurring at seemingly random positions, the scale structure and thickness are similar at all sample positions, as shown in Figure 9.

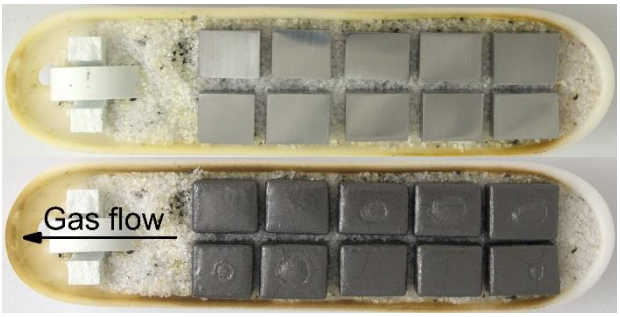

Figure 8. Cr-Mn steel before (top) and after (bottom) non-isothermal oxidation at 1200 °C, 15 min, 6 L/min.

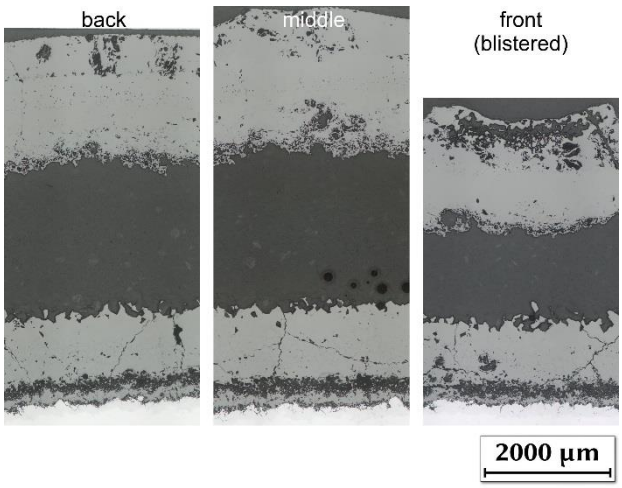

Figure 9. Comparison of scale structures across samples from Figure 8, 10° taper section.

3.2 Oxide scale structure after reheating

For the Si alloyed steel examined in this work, the structure of the scale strongly depends on the isothermal holding temperature, especially in relation to the binary fayalite-wuestite (Fe_2SiO_4-FeO) eutectic at about 1177 °C and the ternary hercynite-fayalite-wuestite ($FeAl_2O_4$-Fe_2SiO_4-FeO) eutectic at about 1148°C [15].

Figure 10 shows a sample oxidized at 1100 °C furnace temperature, resulting in the samples being slightly below the eutectic temperature. There are 3 different regions visible: the base steel, an internal scale containing oxides of Fe, Si and Al, and the external scale consisting solely of Fe oxides, specifically wuestite and magnetite. Hematite was only visible on

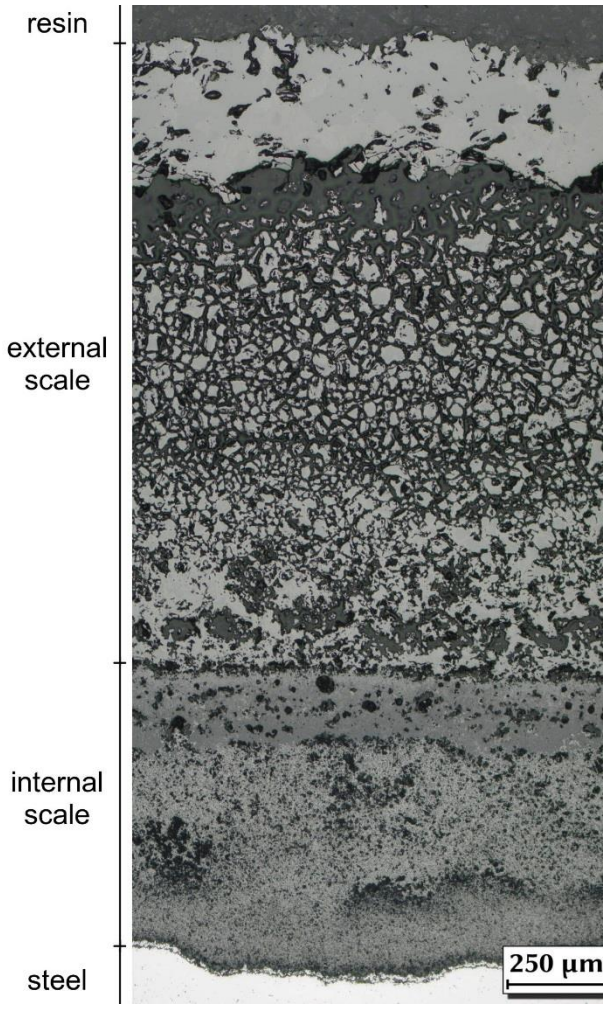

Figure 10. Scale structure of a Si-steel sample oxidized at 1100 °C, 30 min, 10° taper section.

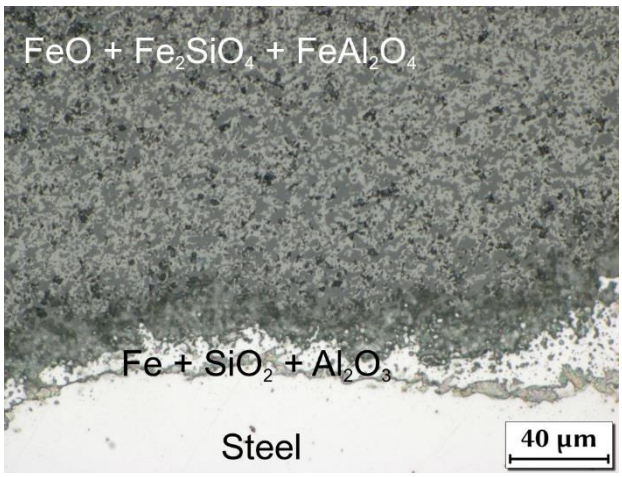

Figure 11. Metal-scale-interface of the Si-steel sample in Figure 10, 10° taper section.

the outside of the scale in cases where separation of the scale during oxidation occurred. The metal-scale-interface is shown magnified in Figure 11. At the interface, there is a zone of mostly pure iron with embedded Si- and Al oxides, as can be seen in the EDS spot analyses in Figure 12. This can be explained by Fe having a certain solubility for oxygen [14], allowing the more oxygen-affine elements Si and Al in the alloy to form oxides and precipitate at the oxidation front, leaving behind the pure iron. As more oxygen is transported into the steel, the solubility limit in Fe is reached and formation of wuestite occurs, enveloping SiO_2 and Al_2O_3 to form Fe_2SiO_4 and $FeAl_2O_4$. The original steel surface before oxidation lies between the internal and the external scale, which was also verified by sputtering samples with gold as a marker before oxidation. Below 1120 °C furnace temperature, no oxides of Si or Al were found in the external scale, as can be seen in the EDS analysis in Figure 13.

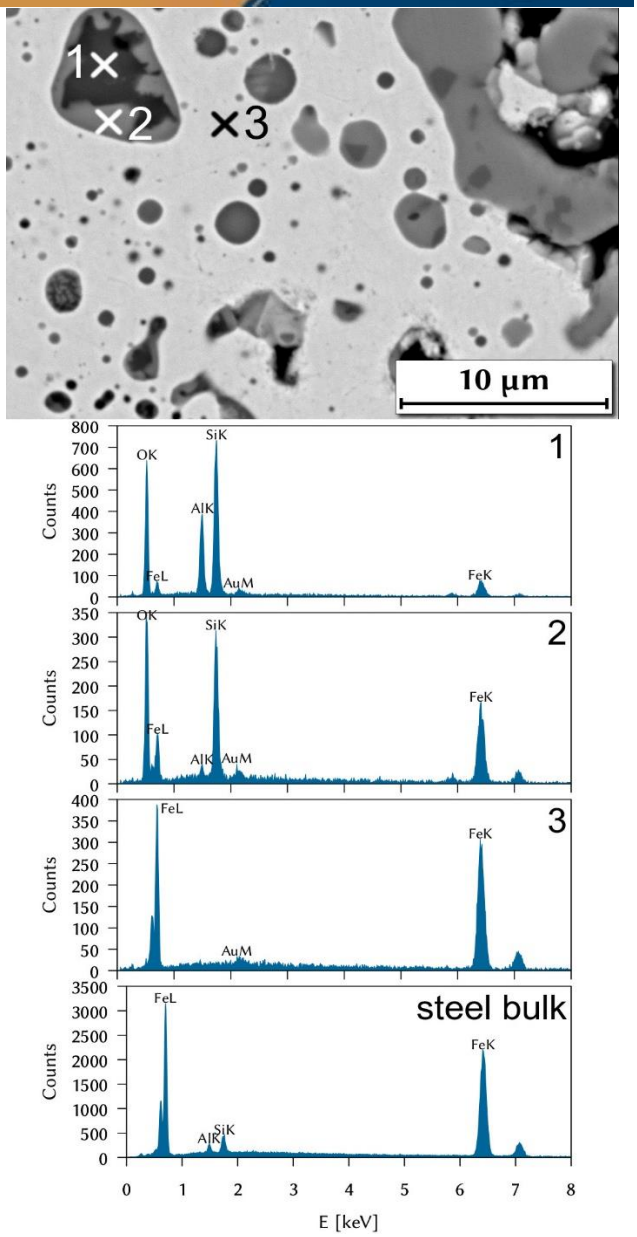

Figure 12. BSE image of the interfacial region with EDS spots and the steel bulk for comparison.

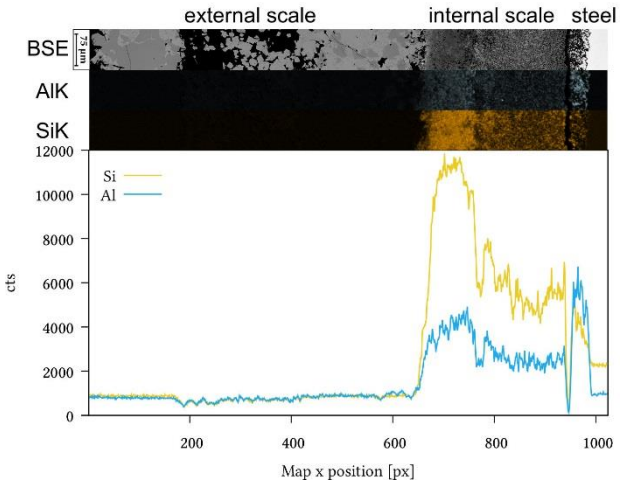

Figure 13. EDS map and line profiles of an Si-steel oxidized at 1050°C, 15 min, 10° taper section.

When oxidizing the samples at a furnace temperature of 1120 °C, the scale takes on a completely different appearance, shown in Figure 14. Parts of the internal scale consisting of FeO, Fe_2SiO_4 and Fe_2AlO_4 seem to have melted and infiltrated the external scale, leaving behind a void near the metal-scale interface mostly filled with resin after cold mounting under vacuum. By formation of the liquid phase, the oxidation rate is increased very much, resulting in a visibly thicker oxide scale despite the shorter isothermal holding time when compared to Figure 10. Figure 15 shows an EDS map of the eutectic area. Both the ternary eutectic containing hercynite, fayalite and wuestite as well as the binary fayalite-wuestite eutectic can be seen. An EDS analysis of the external scale showing the infiltration with the eutectic can be seen in Figure 16. Interestingly, $FeAl_2O_4$ crystals surrounded by what appears to be a hercynite-wuestite eutectic can be seen.

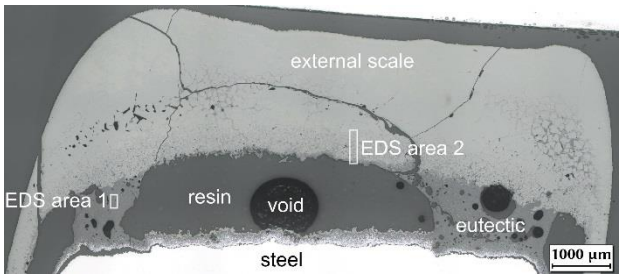

Figure 14. Overview over a Si-steel sample oxidized at 1120 °C, 15 min, 10° taper section.

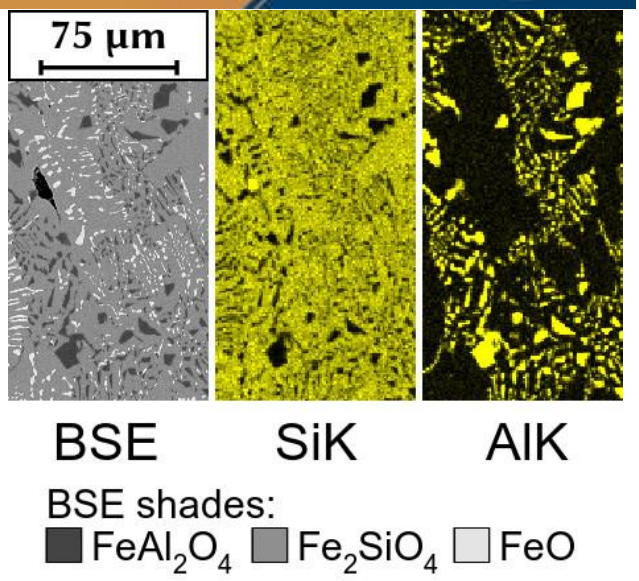

Figure 15. BSE and EDS analysis of the eutectic (EDS area 1 in Figure 14).

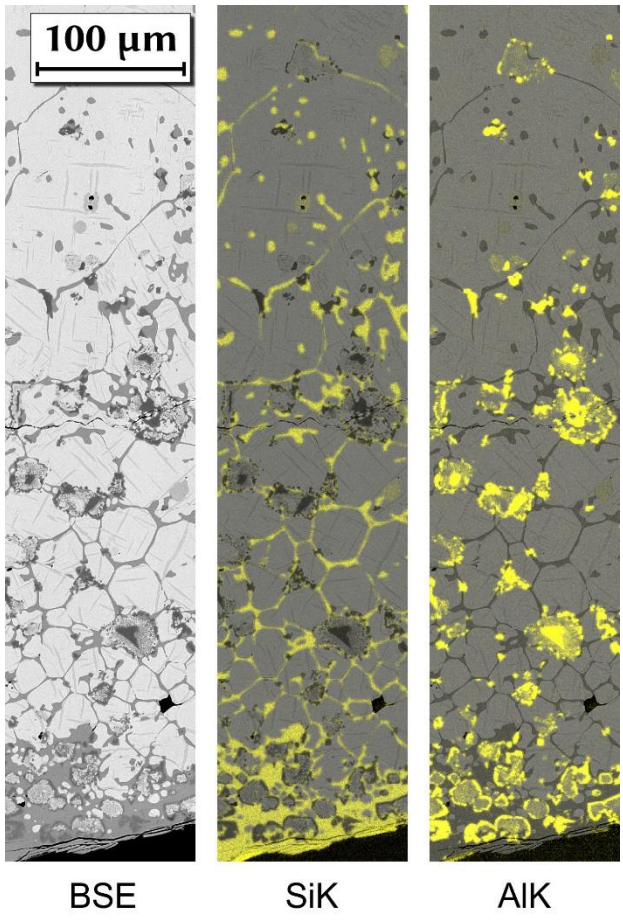

Figure 16. BSE and EDS analysis of the external scale (EDS area 2 in Figure 14).

The formation of liquid phases at a furnace temperature of 1120 °C suggests that the samples are in fact at a higher temperature due to the exothermic nature of the

oxidation reactions. With the ternary eutectic as the lowest melting composition in the system $FeAl_2O_4$-Fe_2SiO_4-FeO at 1148 °C and no indications for the presence of other elements causing a lower melting point, such as P, it can be assumed that the actual sample temperature is about 30–60 K above the temperature measured in the furnace tube. For isothermal oxidation experiments in dry N_2-O_2 mixtures starting at 1100 °C, Abuluwefa et al. [7] report temperature difference spikes of up to 100 K depending on the oxygen content in the atmosphere used, which drop to about 20 K after roughly 10 minutes. Based on this data alone, it is difficult to say how pronounced this effect is for the non-isothermal experiments in this work. However, with the overheating of the samples being dependent on the rate of oxidation, it seems likely that the formation of liquid phase is also self-accelerating by causing a higher scaling rate.

For experiments at 1120 °C, especially at longer holding times, the adhesion of the scale to the substrate often failed during the experiment, resulting in an overoxidized scale with high amounts of hematite due to the interrupted transport of Fe cations through the scale. An example is shown in Figure 17. A possible explanation is that the liquid phase formed near the metal-scale interface infiltrates the external scale through capillary action, resulting in insufficient liquid phase at the interface to keep the scale in contact with the steel.

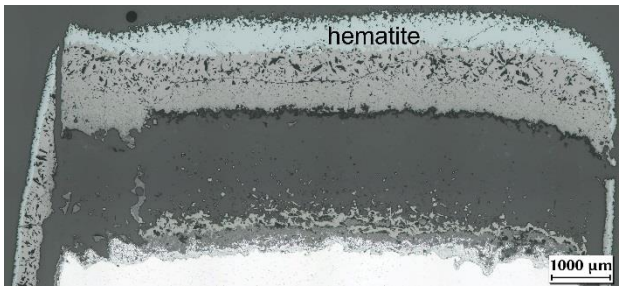

Figure 17. Overview of a Si-steel sample oxidized at 1120 °C, 15 min, 10° taper section.

An example for which the furnace temperature is above both eutectic temperatures at 1220 °C can be seen in Figure 18. In contrast to the sample oxidized at 1120 °C, shown in Figures 14–16, no traces of the hercynite-wuestite eutectic were found, but only the fayalite-wuestite and the ternary hercynite-fayalite-wuestite eutectic. Scale adhesion is also improved due to the larger amount of liquid phase formed. Figure 19 shows EDS maps and line profiles derived from them, with the external scale once more having been infiltrated by the liquid oxides.

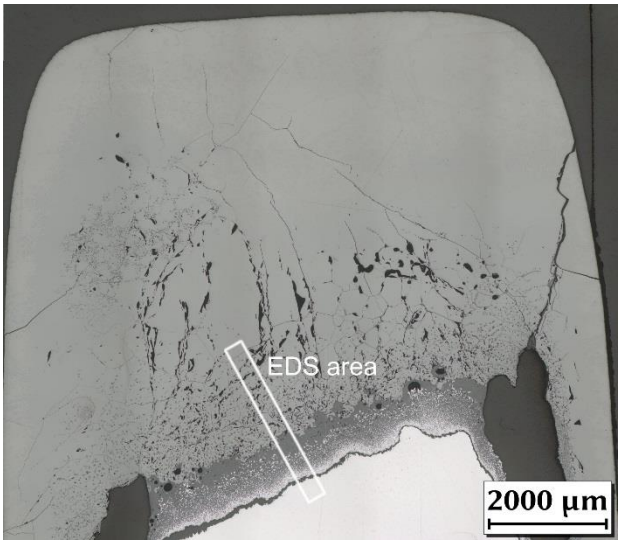

Figure 18. Overview of a Si-steel sample oxidized at 1220 °C, 30 min, 10° taper section.

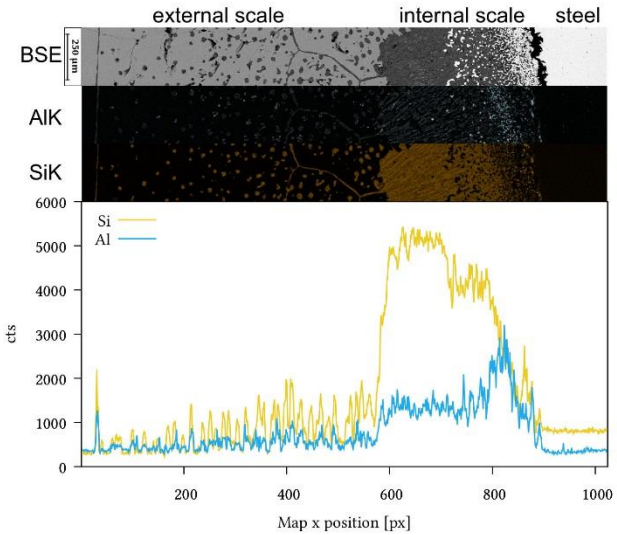

Figure 19. EDS map and line profiles of the sample in Figure 18 (1220°C, 30 min, 10° taper section).

3.3 Simulation of Internal Oxidation

In the simulations performed, a recurring pattern was the formation of bands enriched with hercynite and fayalite during the heating phase. These Si- and Al-rich bands are also visible in the sub-eutectic samples from the oxidation experiments, e.g. in Figures 13 and 20. At the internal oxidation front, a thin band of glassy SiO_2 and Al_2O_3 can be seen as well (see Figure 11).

The simulation result most closely resembling the conditions for the sample in Figure 20 can be seen in Figure 21. Due to aforementioned overheating of the samples caused by oxidation, the simulation temperature was set 60 °C above the furnace temperature in the experiment. While a quantitative comparison is difficult due to the formation of wuestite missing in the simulation, the enrichment of Fe_2SiO_4 and the formation of Al_2O_3 and SiO_2 at the front can be seen.

Based on the simulations performed in Figure 22 for two isothermal holding steps with a heating step in between, it was found that the introduction of a second heating ramp should also cause the formation of a second Si/Al rich band. The corresponding experiment can be seen in Figure 23, indeed showing the additional band.

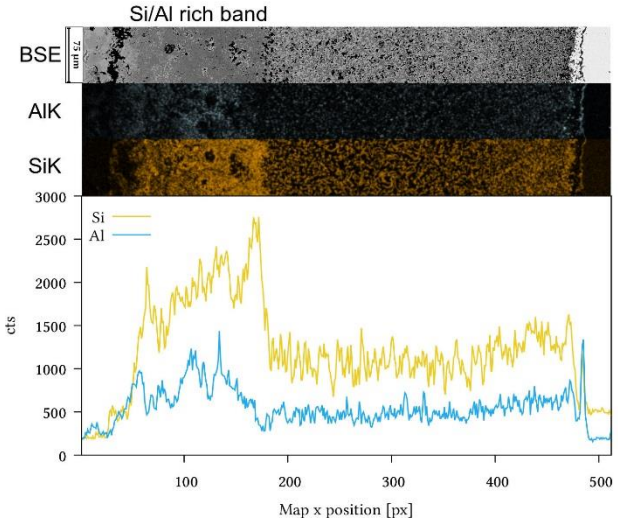

Figure 20. EDS map and line profiles of the Si-steel oxidized at 1100 °C, 30 min, 10° taper section.

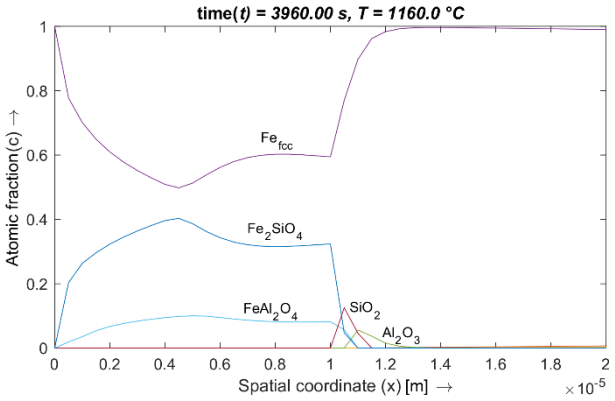

Figure 21. Simulation result for heating from 800 °C to 1160 °C with 10 K/min and holding for 30 min.

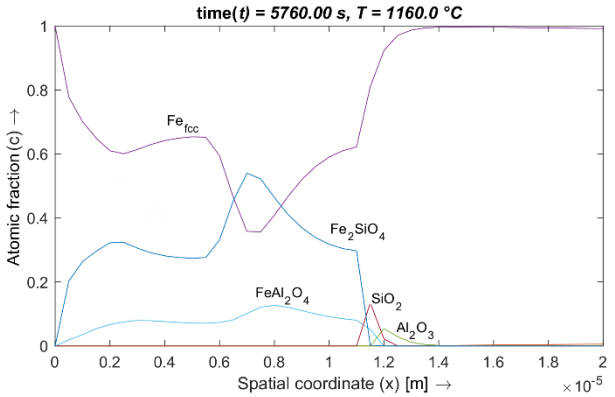

Figure 22. Simulation result for heating from 800 °C to 1060 °C with 10 K/min, holding 30 min, heating to 1160 °C with 10 K/min and holding for 30 min.

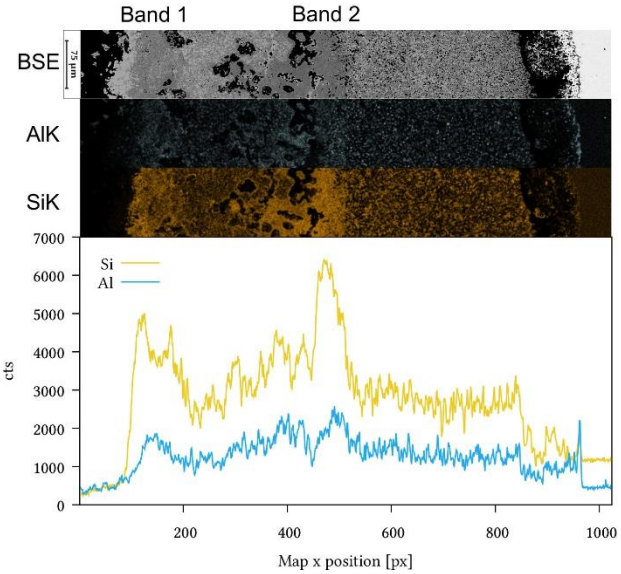

Figure 23. EDS map and line profiles of the Si-steel oxidized at 1000 °C and 1100 °C for 30 min each, 10° taper section.

A possible explanation of this phenomenon can be found in the activation energies of diffusion for the elements involved. First,

the diffusion coefficients of Si and Al are very similar, causing them to behave alike. While O diffuses much faster than Si and Al in Fe at these temperatures, the activation energy for the diffusion of Si and Al is about twice as high, resulting in their diffusion coefficients rising much faster with temperature than that of O. This results in more Si and Al being transported from the steel bulk to the reaction front during heating, causing more oxides to form. At the holding temperature, an equilibrium is reached, and the mass flow of Si and Al decreases again. While the solubility of O in Fe also increases with rising temperature, it is not enough to compensate the change of diffusion with respect to temperature.

4 CONCLUSION

1. For oxidation experiments with multiple or larger samples, one has to make sure to provide enough oxidant flow in relation to the oxidation reaction rate. Insufficient supply will cause changes in the atmosphere between the front and back samples, resulting in different scale morphologies.

2. The scale structure of the Si steel was found to be highly dependent on the oxidation temperature. Liquid phases, which are responsible for most changes in the morphology, were first observed at a furnace temperature of 1120 °C, despite the lowest melting ternary eutectic being at 1148 °C [15]. A possible explanation could be overheating of the samples due to the reaction heat of oxidation, as reported by Abuluwefa et al. [7].

3. Below the eutectic temperature, Si- and Al-rich bands were observed in the internal scale, corresponding to the heating phases in the experiments. Simulations suggest a relationship to the proportion of the activation energies of diffusion of O and Si/Al.

4. At the metal-scale interface, a zone of internal oxides of Si and Al in mostly pure Fe was found, implying a certain solubility of O in Fe, as suggested by Swisher and Turkdogan [14].

Acknowledgments

The authors gratefully acknowledge the funding support of K1-MET GmbH, metallurgical competence center. The research program of the competence center K1-MET is supported by COMET (Competence Center for Excellent Technologies), the Austrian program for competence centers. COMET is funded by the Federal Ministry for Transport, Innovation and Technology, the Federal Ministry for Science, Research and Economy, the province of Upper Austria, Tyrol, and Styria, the Styrian Business Promotion Agency.

REFERENCES

1 Fukagawa T, Okada H, Maehara Y. Mechanism of Red Scale Defect Formation in Si-added Hot-rolled Steel Sheets. ISIJ International. 1994; 34(11): 906–911

2 Melfo W, Bolt H, Rijnders M, Staalman D, Benito Castro C, Crowther D, Jana B. Experimental Study on Primary Scale Formation and Descalability on Steels Containing Ni and Ni+Si. ISIJ International. 2013; 53(5): 866–873

3 Fukagawa T, Okada H, Maehara Y, Fujikawa H. Effect of Small Amount of Ni on Hydraulic-descaling-ability in Si-added Hot-rolled Steel Sheets. Tetsu-to-Hagane. 1996; 82(1): 63–68

4 Chen RY, Yuen WYD. Oxide scales on hot-rolled steel strips. Developments in High Temperature Corrosion and Protection of Materials. 2008: 192–252

5 Chen RY, Yuen WYD. Effects of the Presence of Water Vapour on the Oxidation Behaviour of Low Carbon-Low Silicon Steel in 1 % O_2-N_2 at 1073 K. Oxidation of Metals. 2013; 79(5): 655–678

6 Sheasby JS, Boggs WE, Turkdogan ET. Scale growth on steels at 1200 °C: rationale of rate and morphology. Metal Science. 1984; 18(3): 127–136

7 Abuluwefa HT, Guthrie RIL, Ajersch F. The effect of oxygen concentration on the oxidation of low-carbon steel in the temperature range 1000 to 1250 °C. Oxidation of Metals. 1996; 46(5): 423–440

8 Sobotka C, Antrekowitsch H, Schnideritsch H. The Influence of Oxygen-Enriched Burner Systems on the Scale Formation of Steel Alloys During Heating Processes. AISTech 2014 Proceedings. 2014: 3115–3131

9 Abuluwefa HT, Gutrie RIL, Ajersch F. Oxidation of low carbon steel in multicomponent gases: Part I. Reaction mechanisms during isothermal oxidation. Metallurgical and Materials Transactions A. 1997; 28(8): 1633–1641

10 Chen RY, Yuen WYD. Examination of Oxide Scales of Hot Rolled Steel Products. ISIJ International. 2005; 45(1): 52–59

11 Auinger M, Praig VG, Linder B, Danninger H. Grain boundary oxidation in iron-based alloys, investigated by ^{18}O enriched water vapour – The effect of mixed oxides in binary and ternary Fe–{Al, Cr, Mn, Si} systems. Corrosion Science. 2015; 96: 133–143

12 Bott JH, Yin H, Sridhar S, Auinger M. Theoretical and experimental analysis of selective oxide and nitride formation in Fe–Al alloys. Corrosion Science. 2015; 91: 37–45

13 Birks N, Meier GH, Pettit FS. Introduction to the High-Temperature Oxidation of Metals. 2nd Edition. Cambridge University Press; 2006

14 Swisher JH, Turkdogan ET. Solubility, Permeability, and Diffusivity of Oxygen in Solid Iron. Transactions of the Metallurgical Society of AIME. 1967; 239(4): 426–431

15 Levin EM, Robbins CR, McMurdie HF. Phase diagrams for ceramists. Columbus, Ohio: Reser MK; 1964.